Rovibronically Selected and Resolved Two-Color Laser Photoionization and Photoelectron Study of the Iron Carbide Cation†

Y.-C. Chang,‡,§ C.-S. Lam,‡ B. Reed,‡ K.-C. Lau,|| H. T. Liou,§ and C. Y. Ng*,‡

Department of Chemistry, University of California, Davis, Davis, California 95616, Institute of Atomic and Molecular Sciences, Academia Sinica, Taipei, Taiwan, and Department of Biochemistry and Chemistry, City University of Hong Kong, Kowloon, Hong Kong

Received: December 8, 2008; Revised Manuscript Received: January 3, 2009

By using a two-color laser excitation−photoionization scheme, we have obtained rovibronically selected and resolved state-to-state pulsed field ionization−photoelectron (PFI-PE) bands for $FeC^+(X^2\Delta_{5/2}; v^+=0-2, J^+)$, allowing unambiguous rotational assignments for the photoionization transitions. The finding of the $J^+ = 5/2$ level as the lowest rotational state confirms that the ground FeC^+ ion state is of $^2\Delta_{5/2}$ symmetry. The observed changes in total angular momentum upon photoionization of FeC are $|\Delta J^+| = |J^+ - J'| \leq 3.5$, indicating that the photoelectron orbital angular momentum is limited to $l \leq 3$. This observation is also consistent with the conclusion that the photoionization involves the removal of an electron from the highest occupied molecular orbital of the π-type. The ionization energy, IE = 61243.1 ± 0.5 cm^{-1} (7.59318 ± 0.00006 eV), for the formation of FeC^+ ($X^2\Delta_{5/2}$, $v^+=0$; $J^+=5/2$) from FeC ($X^3\Delta_3$, $v''=0$; $J''=3$), the rotational constants, $B_e^+ = 0.7015 \pm 0.0006$ cm^{-1} and $\alpha_e^+ = 0.00665 \pm 0.00036$ cm^{-1}, and the vibrational constants, $\omega_e^+ = 927.14 \pm 0.04$ cm^{-1} and $\omega_e^+\chi_e^+ = 6.35 \pm 0.04$ cm^{-1}, for $FeC^+(X^2\Delta_{5/2})$ determined in the present study are compared to the recent state-of-the-art ab initio quantum chemical calculation at the C-MRCI+Q level of theory. The large deviation (0.49 eV) observed between the present experimental IE value and the C-MRCI+Q theoretical IE prediction highlights the great need for the further development of ab initio quantum theoretical procedures for more accurate energetic predictions of transition metal-containing molecules.

I. Introduction

Understanding the bonding between transition metals and main group elements is important in many areas of science, including organometallic chemistry, catalysis, and astrophysics.[1−3] The stability of the nuclei of 3d transition metals makes these elements and their hydrides, carbides, and oxides important astrochemical species.[1−4] Many transition metal compounds are known industrial catalysts.[5] Partly due to the need for understanding of the mechanisms and intermediates involved in catalytic processes and for modeling of the solar spectra of stellar objects and interstellar medium, the spectroscopic studies of gaseous transition metal-containing molecules represent an active research field in chemical physics.[1,2,6−12] However, the previous high-resolution spectroscopic studies have mostly focused on neutral[1,2,4,6−8] transition metal hydrides, carbides, and oxides. The high-resolution spectroscopic studies on their cations[9−11] remain sparse.

While standard quantum computation packages can be used routinely to calculate reliable energetic information, such as ionization energies (IEs) and 0 K bond dissociation energies (D_0), of molecules of the main group elements,[13−15] a different scenario exists for the theoretical treatment of transition metal-containing molecules.[1] The difficulty in obtaining reliable structural and energetic predictions of transition metal-containing species arises from the existence of many unpaired d-subshell electrons of the transition metal atom(s), which can give rise to a large number of low-lying electronic states of different multiplicities. Thus, the extent of electron correlation and electronic interaction required for the reliable theoretical treatments of transition metal compounds is significantly greater than that for molecules of the main-group elements. The further development of reliable quantum chemical treatments for transition metal compounds would require the benchmarking of the theoretical predictions by precise experimental energetic determinations of these compounds and their ions.

The transition metal carbides provide an interesting and important set of molecules for detailed experimental and theoretical study, because of the significance of the transition metal−carbon bond in catalysis, biological processes, and organometallic chemistry. This report presents the results of a rotationally selected and resolved state-to-state photoionization and photoelectron study of iron carbide (FeC) using the two-color visible−ultraviolet (UV) laser excitation−ionization scheme. The selection of the FeC/FeC^+ system is partially motivated by the recent state-of-the-art high-level ab initio quantum chemical calculations[16,17] based on the multireference variation method (MRCI) and the lack of precise experimental IE and D_0 determinations for FeC and FeC^+.

This two-color visible−ultraviolet (UV) scheme takes advantage of the fact that nearly all transition metal-containing species possess long-lived low-lying electronic states.[1,2,6−10,12] Furthermore, many of the low-lying neutral electronic states have been characterized in detail in previous spectroscopic studies.[2,6−10,12] Thus, a transition metal-containing species, such as FeC, in a selected rovibronic state can be readily selected by visible laser excitation prior to UV laser photoionization efficiency (PIE) and pulsed field ionization−photoelectron (PFI-PE) measurements, allowing complete rotationally resolved state-to-state photoionization transitions to be identified. The two-color photoionization scheme not only can

† Part of the "George C. Schatz Festschrift".

* To whom correspondence should be addressed. E-mail: cyng@chem.ucdavis.edu.

‡ University of California.

§ Institute of Atomic and Molecular Sciences.

|| City University of Hong Kong.

10.1021/jp810797v CCC: $40.75
Published on Web 02/09/2009

overcome the spectral congestion problem as demonstrated in our recent two-color infrared−vacuum ultraviolet PFI-PE studies,[18−26] but also allowed the selection of a molecule of interest without interference from other impurity species produced in the laser ablation source. Although only the experiment for the FeC/FeC^+ system is presented in this report, the two-color visible−UV PIE and PFI-PE schemes described here should be generally applicable for other diatomic and polyatomic transition metal-containing molecules.

Due to the difficulty in preparing transition metal-containing molecules in the gas phase with sufficiently high intensities, only the origin photoelectron bands of several transition metal oxide cations (VO^+ and YO^+, and TiO^+, ZrO^+, NbO^+, and MoO^+) have been examined by the high-resolution PFI-PE or PFI-photoion detection scheme.[9−11] As described below, we have increased the intensities of transition metal-containing species at the photoionization region compared to those obtainable in previous experiments[7,8,11,12] by reducing the distance between the laser ablated transition metal source and the photoionization region. This improvement is expected to allow the PIE and PFI-PE studies of many minor transition metal-ligated species formed in the laser ablated transition metal source, which could not be observed in previous experiments.

II. Experimental Methods

The experimental arrangement and procedures of using the photoion−photoelectron apparatus for the two-color laser photoionization efficiency (PIE) and PFI-PE measurements have been described in detailed previously.[18−28] Briefly, the apparatus consists of two tunable dye lasers pumped by a single injection seeded Nd:YAG laser, a laser ablation metal beam source for the production of a supersonic beam of FeC, a time-of-flight (TOF) mass spectrometer for ion detection, and a TOF electron spectrometer for PFI-PE detection. Both the ion and electron detectors were constructed of a dual set of microchannel plates (MCPs).

A Smalley-type laser ablation beam source[29] was used to prepare and introduce gaseous FeC molecules into the photoionization region in the form of a supersonic beam of FeC seeded in He. The gaseous Fe atoms and minor Fe clusters were produced by ablation of a rotating and translating carbon steel rod (McMaster-Carr, 0.4% of carbon) by using the second harmonic (532 nm) output of a Nd:YAG laser (Continuum Inc., Surelite-1-30) operating at 30 Hz and a pulse energy of ∼1 mJ. The plasma plume of Fe species thus formed was timed to be carried by a pulsed gas stream of He doped with 3% of methane (CH_4) to pass through a stainless steel channel (diameter = 2 mm, length = 1 cm) before supersonic expansion to form a pulsed beam of FeC seeded in He. The pulsed He/CH_4 gas stream was produced by a piezoelectric valve operating at 30 Hz and a stagnation pressure of ∼40 psi. The gaseous FeC molecules were assumed to be produced by the reactions of the Fe plasma plume and CH_4. The entrenchment of the FeC gaseous plume by He in the stainless steel channel, followed by the supersonic expansion, had the function of cooling excited Fe and Fe-containing species by collisions. The FeC beam thus prepared was skimmed by a conical skimmer (diameter = 2 mm) prior to intersecting perpendicularly with the visible (ω_1) and UV (ω_2) laser beams at the photoionization region. To minimize the background noise in photoion and PFI-PE detections, we found that it was important to removal the ionic species emerging from the stainless steel channel using a pair of repeller plates installed between the exit of the stainless steel channel and the skimmer. The major difference in using the laser ablation metal source in the present study compared to those in previous studies reported in the literature was that the laser ablation metal source was situated ∼7 cm from the laser photoexcitation and photoionization region in the present experiment, whereas a distance of 15−25 cm was used in the previous studies.

The visible (ω_1 = 18 520−20 833 cm^{-1}) and UV (ω_2 = 40 650−44 248 cm^{-1}) frequencies required were generated by two dye lasers, which were pumped by an identical injection seeded Nd:YAG laser (Quanta-Ray Model GCR-290, 30 Hz) at the third harmonic output of 355 nm. The ω_1 and ω_2 laser beams were merged by a dichroic mirror before entering the entrance arm of a monochromator through an MgF_2 window. By setting the monochromator in the zeroth order, both the ω_1 and ω_2 laser beams were focused and guided to intersect the FeC molecular beam at the photoexcitation/photoionization region at 90°.

In this two-color photoionization study, the ω_1 pulse was employed to excite FeC from a J'' rotational level of its ground $X^3\Delta_3$ state to a J' rotational level of the excited $^3\Delta_3$ intermediate state at ∼493 nm.[6,7] The application of the ω_2 photoionization laser pulse was delayed by ∼5 ns with respect to the ω_1 laser pulse. Both the ω_1 and ω_2 frequencies were calibrated by wavemeters to within an uncertainty of ±0.04 cm^{-1} (fwhm) during the experiment. For photoion measurements, a dc field of 40−60 V/cm was applied in the photoionization region to extract photoions into the TOF mass spectrometer for mass analysis and to be detected by the ion MCP detector. For PFI-PE measurements, a dc field of 0.1 V/cm was used to disperse prompt electrons away from the electron TOF spectrometer, and a pulsed electric field of 0.5−1.0 V/cm (width = 40 μs) was applied after a 1 μs delay with respect to the ω_2 photoionization laser pulse for PFI as well as for extraction of the resulting PFI-PEs toward the electron MCP detector.

Delayed pulse generators (Stanford research system, DG535) were used to synchronize the timing of turning on the piezoelectronic pulse valve, the ablation laser, the visible excitation laser, the UV photoionization laser, and the PFI field. The signal from the ion or electron MCP detector was amplified by a fast preamplifier (Stanford research system, SR445) before detection by a gated integrator (Stanford research system, SR250). The output from the boxcar integrator was fed into an A/D converter before processing by a personal computer. The ion or electron signal was generally averaged for 15−60 shots at each scanning laser frequency. All ion and PFI-PE spectra presented here represent the average of four independent scans and have been normalized by the scanning visible ω_1 or UV ω_2 laser power.

III. Results and Discussion

Many neutral electronic bands of FeC have been investigated previously by means of laser-induced fluorescence[6] (LIF) and two-color visible-excimer laser photoionization.[7] Among these neutral electronic bands, we have chosen the FeC($^3\Delta_3$) ← FeC($X^3\Delta_3$) band at 493.0 nm for the preparation of the excited FeC($^3\Delta_3$; v', J') states as the intermediate rovibronic levels for photoionization study. This electronic band has been well analyzed previously.[6,7] Furthermore, the rotational levels of the excited FeC($^3\Delta_3$) intermediate state were found to have sufficiently long lifetimes (∼65 ns)[6,7] for two-color photoionization measurements. Using a tunable visible laser to populate discrete intermediate rovibronic levels of FeC, followed by the 193.3 nm ArF excimer photoionization probe, Brugh and Morse have reported a value of 7.74 ± 0.09 eV (62 427 ± 726 cm^{-1}) for the IE of FeC.[7] Assuming this IE value to be correct, the UV ω_2 frequency needed to ionize FeC in a rotational level of the

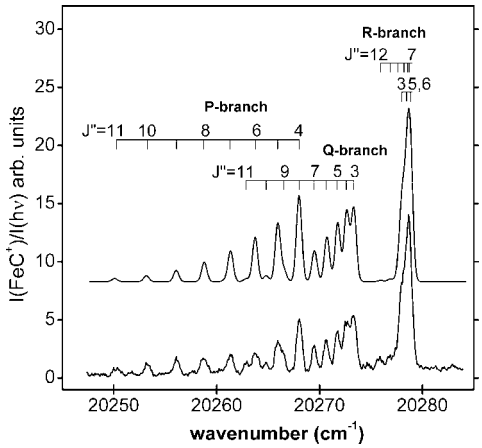

Figure 1. Lower spectrum: The FeC($^3\Delta_3$; v'=0, J') ← FeC($X^3\Delta_3$; v''=0, J'') electronic band recorded by fixing ω_2 = 42 006.3 cm^{-1} and measuring the FeC$^+$ ion intensity as a function of ω_1 frequency in the range of 20 247−20 284 cm^{-1}. Upper spectrum: The best simulated spectrum obtained based on the standard rovibronic transition formula (eq 1), the assumption of a Gaussian instrumental profile (fwhm = 0.5 cm^{-1}) for the rotational transitions, and a Boltzmann rotational distribution with a rotational temperature of 28 K for the FeC($X^3\Delta_3$; v''=0) ground state.

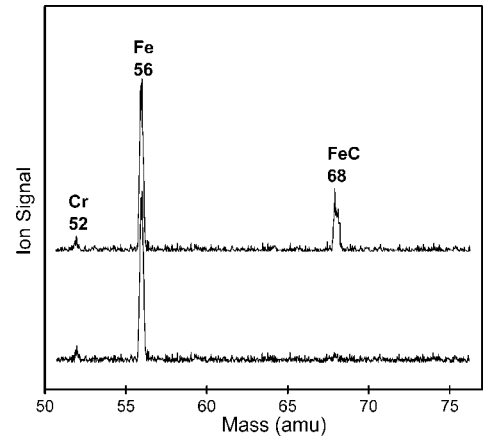

Figure 2. The TOF mass spectrum (upper spectrum) observed with ω_1 = 20 278.67 cm^{-1} (the maximum of the R-branch in Figure 1) and ω_2 = 42 006.3 cm^{-1}. This spectrum reveals the $^{56}Fe^+$ ion peak at mass 56 and the FeC$^+$ ion peak at mass 68. The lower TOF spectrum was observed with the ω_1 laser beam off and ω_2 = 42 006.3 cm^{-1}.

intermediate $^3\Delta_3$ state is expected to be higher than ∼42 143 cm^{-1}. The latter UV frequency can readily be generated by frequency doubling of the visible output of a dye laser.

By fixing ω_2 at 42 006.3 cm^{-1} and measuring the FeC$^+$ ion intensity as a function of ω_1 frequency in the range of 20 245−20 285 cm^{-1}, we have recorded the $^3\Delta_3$ ← $X^3\Delta_3$ electronic band as shown in the lower spectrum of Figure 1. The structure of this spectrum is similar to that observed previously with the LIF method, except that the observed rotational line width of 0.5 cm^{-1} (full-width at half-maximum, fwhm) of this spectrum is broader than that of the LIF spectrum.[6] The fact that the optical bandwidth (0.04 cm^{-1}, fwhm) of the ω_1 laser used is significantly narrower than the rotational line width indicates that power broadening is operative in the present measurement. Using the standard formula: $G(v) = \omega_e(v + 1/2) - \omega_e\chi_e(v + 1/2)^2$ for vibrational energy and $F(J') = B'J'(J' + 1)$ for rotational energy, the transition energy for the rovibronic transition, FeC($^3\Delta_3$; v'=0, J') ← FeC ($X^3\Delta_3$, v'' = 0; J'') can be written as

$$v = v_{00} + B'J'(J' + 1) - B''J''(J'' + 1) \qquad (1)$$

Here, $v_{00} = \Delta T_{e'e''} + (\omega_{e'}/2 - \omega_{e'}\chi_{e'}/4) - (\omega_{e''}/2 - \omega_{e''}\chi_{e''}/4)$, where $\omega_{e'}$ and $\omega_{e'}\chi_{e'}$ ($\omega_{e''}$ and $\omega_{e''}\chi_{e''}$) are the respective harmonic frequency and anharmonicity constant for the excited (ground) state, $\Delta T_{e'e''}$ is the energy separation between the potential minimum of the ground state and that of the excited state, and B' (B'') is the rotational constant for the excited (ground) state. The B'' constant for the Fe($X^3\Delta_3$) ground state is known to be 0.669 643 18 cm^{-1}.[4] By assuming a Gaussian instrumental profile of 0.5 cm^{-1} (fwhm) for the rotational transitions and a Boltzmann distribution of rotational populations for the neutral ground state, we have simulated the lower spectrum of Figure 1 according to eq 1. The best simulated spectrum (upper spectrum of Figure 1) gives a rotational temperature of 28 K for the FeC beam, the origin v_{00} = 20 274.34 ± 0.04 cm^{-1} for the FeC($^3\Delta_3$) ← FeC ($X^3\Delta_3$) electronic band, and the rotational constant B' = 0.5832 ± 0.0002 cm^{-1} for the intermediate FeC($^3\Delta_3$) state. These results are in agreement with the values[6,7] of v_{00} = 20273.6 cm^{-1} and B' = 0.5813 cm^{-1} reported previously[6] in the LIF study. Since the latter LIF study claimed an error limit of 1 cm^{-1} for the energy calibration, we may conclude that the observed discrepancy of 0.74 cm^{-1} between the v_{00} value of the present experiment and that of the LIF study is within the error of frequency calibration of the LIF study. On the basis of the spectral simulation, we have also assigned the $P(J'')$, $Q(J'')$, and $R(J'')$ rotational branch transitions as marked on top of Figure 1. The observation of the $Q(3)$ and $P(4)$ rotational transitions as the lowest member of the respective Q- and P-branches indicates that the angular momentum for the intermediate state is $\Omega' = 3$, i.e., the electronic band is confirmed to correspond to the FeC($^3\Delta_3$) ← FeC($X^3\Delta_3$) transition.

The TOF mass spectrum obtained with ω_1 fixed at 20 278.67 cm^{-1} (the maximum of the R-branch in Figure 1) and ω_2 at 42 006.3 cm^{-1} is shown as the upper spectrum in Figure 2. This spectrum reveals predominantly two ion peaks, namely, the $^{56}Fe^+$ ion peak at mass 56 and the FeC$^+$ ion peak at mass 68. When the ω_1 laser beam was blocked from entering the photoionization region and ω_2 was set at 42 006.3 cm^{-1}, we observed the lower TOF spectrum of Figure 2, in which the FeC$^+$ ion peak was indiscernible. The Fe$^+$ ion peak observed in this lower TOF spectrum is found to have nearly the same intensity as that of the upper TOF spectrum. This observation indicates that the FeC$^+$ ions are only formed by two-color visible−UV photoionization, whereas the Fe$^+$ ions are produced predominantly by nonresonant two-photon UV photoionization.

Figure 3 depicts the PIE spectrum for FeC$^+$($^2\Delta_{5/2}$; v^+=0−3) in the total photon frequency range of 60 939−64 394 cm^{-1} (bottom frequency scale) obtained by setting ω_1 = 20 278.67 cm^{-1} (the maximum of the R-branch in Figure 1) and scanning ω_2 frequency in the region of 40 661−44 116 cm^{-1} (top frequency scale). The total photon frequency represents the sum of the visible ω_1 and UV ω_2 frequencies. The spectral simulation shows that by setting ω_1 at the maximum of the R-branch of Figure 2, the main rotational states populated are the $J' = 5$ and 6 states with the population ratio of ∼5:4 as estimated based on the Boltzmann distribution for a rotational temperature of 28 K. As shown in Figure 3, the PIE spectrum exhibits sharp step-like onsets at 61 242, 62 155, 63 051, and 63 939 cm^{-1}, giving the frequency spacings between adjacent onsets to be 913, 896, and 888 cm^{-1}. At total photon frequencies below ∼61 240 cm^{-1}, the FeC$^+$ ion intensity is found to be at the noise level, indicating that the lowest energy onset at 61 242 cm^{-1} (7.593 eV) can be assigned as the adiabatic IE of FeC($X^3\Delta_3$). This value is ∼0.15 eV lower than that reported previously.[7]

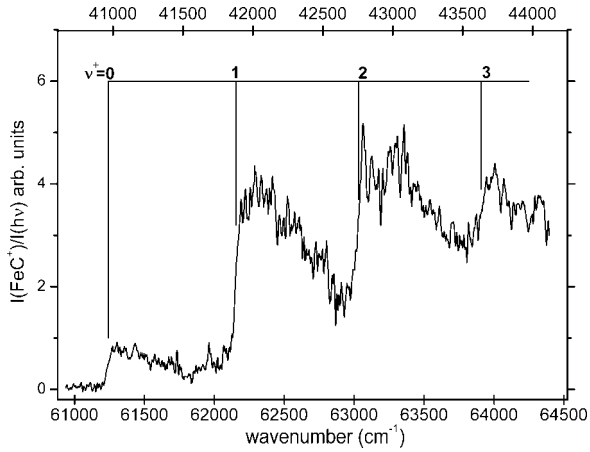

Figure 3. The PIE spectrum for $FeC^+(^2\Delta_{5/2}; v^+=0-3)$ in the total photon frequency range of 60 939−64 394 cm^{-1} (bottom frequency scale) obtained by setting $\omega_1 = 20\,278.67$ cm^{-1} and scanning ω_2 in the region of 40 661−44 116 cm^{-1} (top frequency scale). Sharp step-like PIE onsets are observed at 61 242, 62 155, 63 051, and 63 939 cm^{-1}, which are assigned as the ionization thresholds for $v^+ = 0$, 1, 2, and 3, respectively.

Considering that these frequency spacings determined by the PIE steps are close to the predicted vibrational frequency[17] of 944 cm^{-1} for the $FeC^+(X^2\Delta)$ ground state, we have assigned the PIE steps to be the ionization onsets for the formation of $FeC^+(X^2\Delta_{5/2}; v^+=0,1,2,3)$ from $FeC(X^3\Delta_3; v''=0)$.

The relative Franck−Condon factors (FCFs) for the photoionization transitions $FeC^+(X^2\Delta_{5/2}; v^+=0,1,2,3) \leftarrow FeC(^3\Delta_3; v'=0)$ determined based on the vibrational PIE step heights observed in the PIE spectrum are 0.22, 1.00, 0.53, and 0.28, respectively. The MRCI calculations of Tzeli and Mavridis[16] show that the neutral $FeC(X^3\Delta_3)$ ground state is of multiconfiguration character with the leading electronic configuration $7\sigma^2 8\sigma^2 3\pi^4 1\delta^3 9\sigma^1$, where the 1δ and 9σ orbitals have nearly entirely metal 3d and 4s characters, respectively. Due to the dominantly nonbonding nature of the 9σ, the $FeC^+(X^2\Delta)$ ground state produced from the removal of the electron in this highest occupied 9σ orbital is expected to have a similar bond dissociation energy as that for the neutral ground state. The nonbonding nature of the 9σ orbital also predicts similar IE values for Fe and FeC. The excited $FeC(^3\Delta_3)$ intermediate state has been assigned[6] a mixture of two dominant configurations, $8\sigma^2 3\pi^3 1\delta^3 9\sigma^1 4\pi^1$ and $8\sigma^1 3\pi^4 1\delta^3 9\sigma^1 4\pi^1$. Since these configurations are formed by excitation of an electron from the bonding 3π or 8σ orbital to the antibonding 4π orbital, the Fe−C bond in the excited $FeC(^3\Delta_3)$ state is expected to be much weaker than the neutral ground state. For the bonding between Fe and C, the antibonding 4π orbital is expected to be dominated by the 2p character of the C atom. The $^3\Delta_3$ state at 493 nm is 58 kcal/mol or 2.51 eV above the ground $FeC(X^3\Delta)$ state. We note that only the $29^3\Delta$ state is predicted in the recent high-level ab initio quantum MRCI calculations of Tzeli and Mavridis to lie in the energy range of 50−70 kcal/mol above the ground $FeC(X^3\Delta)$ state. Although the $29^3\Delta$ state is predicted to be ∼10 kcal/mol higher than the $^3\Delta_3$ state of interest here, we may identify the $^3\Delta_3$ state at 493 nm with the $29^3\Delta$ state. According to the MRCI calculations of Tzeli and Mavridis,[16,17] the equilibrium bond distance (r_e = 1.598 Å) for the neutral $FeC(X^3\Delta; v''=0)$ ground state is only slightly longer than that (r_e^+ = 1.557 Å) of the cationic $FeC^+(X^2\Delta; v^+=0)$ ground state. These theoretical r_e and r_e^+ values are consistent with the experimental rotational constants for $FeC(X^3\Delta; v''=0)$[8] and $FeC^+(X^2\Delta; v^+=0)$ (see the discussion below). The measured

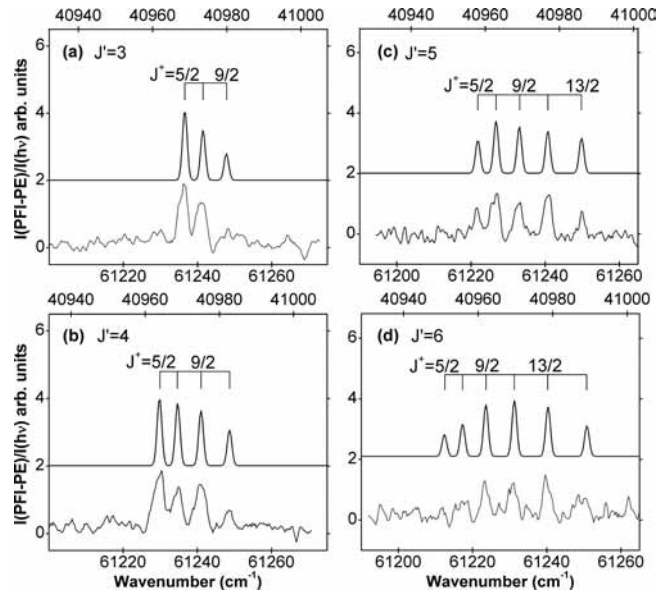

Figure 4. Rotationally selected and resolved PFI-PE spectra (lower spectra) for the formation of $FeC^+(X^2\Delta_{5/2}; v^+=0, J^+)$ from $FeC(^3\Delta_3; v'=0)$ with (a) $J' = 3$, (b) $J' = 4$, (c) $J' = 5$, and (d) $J' = 6$, which were selected by setting the ω_1 frequency at the respective $P(4)$, $P(5)$, $P(6)$, and $P(7)$ transition lines of the spectrum shown in Figure 1 and scanning the ω_2 frequency in the range of 40 935−41 005 cm^{-1} (top frequency scale). The total photon frequency range of 61 190−61 275 cm^{-1} is shown in the bottom frequency scale. The upper spectra are the simulated spectra.

rotational constant B' gives an r_e value of 1.703 Å for the intermediate $FeC(^3\Delta_3; v'=0)$ state, which is significantly larger than those of the $FeC^+(X^2\Delta_{5/2}; v^+=0)$ and $FeC(^3\Delta_3; v''=0)$ states. Thus, the broad Franck−Condon distribution for the $FeC^+(X^2\Delta_{5/2}; v^+=0,1,2,3) \leftarrow FeC(^3\Delta_3; v'=0)$ photoionization transitions observed in the PIE spectrum of Figure 3 is consistent with the large difference in the equilibrium bond distances of $FeC^+(X^2\Delta_{5/2})$ and $FeC(^3\Delta_3)$. Although the unfavorable FCF condition for photoionization via the intermediate $FeC(^3\Delta_3)$ state gives low PIEs at the $v^+=0$ ionization step, it has the advantage of allowing the observation of higher v^+ vibrational bands for $FeC^+(X^2\Delta_{5/2})$.

The rotationally selected and resolved PFI-PE spectra (lower spectra) for the $FeC^+(X^2\Delta_{5/2}; v^+=0, J^+) \leftarrow FeC(^3\Delta_3; v'=0, J'=3,4,5,6)$ photoionization transitions in the total photon frequency range of 61 190−61 275 cm^{-1} (bottom frequency scale) shown in parts a−d of Figure 4 are obtained by setting the ω_1 frequency at the rotational transitions, $P(4)$, $P(5)$, $P(6)$, and $P(7)$, respectively, of the spectrum shown in Figure 1 and scanning the UV ω_2 frequency in the range of 40 935−41 005 cm^{-1} (top frequency scale). The upper spectra shown in Figure 4a−d are the corresponding simulated spectra obtained by assuming an instrumental Gaussian profile with a fwhm of 1.5 cm^{-1} for the rotational transitions. The rotational intensities of the simulated spectra were adjusted to give the best overall fit to the experimental spectra.[20−26] The J^+ rotational levels of the $FeC^+(X^2\Delta_{5/2}; v^+=0)$ ground ion state observed via the selected $J' = 3$, 4, 5, or 6 rotation level of the $FeC(^3\Delta_3; v'=0)$ intermediate state are marked on top of the simulated spectra. Since only a single J' level is selected in these measurements, the $J^+ \leftarrow J'$ transitions are clearly resolved in the PFI-PE spectra, allowing the unambiguous rotational assignments. The least-squares fit according to the standard formula for rotational transitions yields the rotational constant $B_0^+ = 0.6978 \pm 0.0008$ cm^{-1} and the band origin $\nu_{00}^+ = 61\,243.58 \pm 0.03$ cm^{-1} for

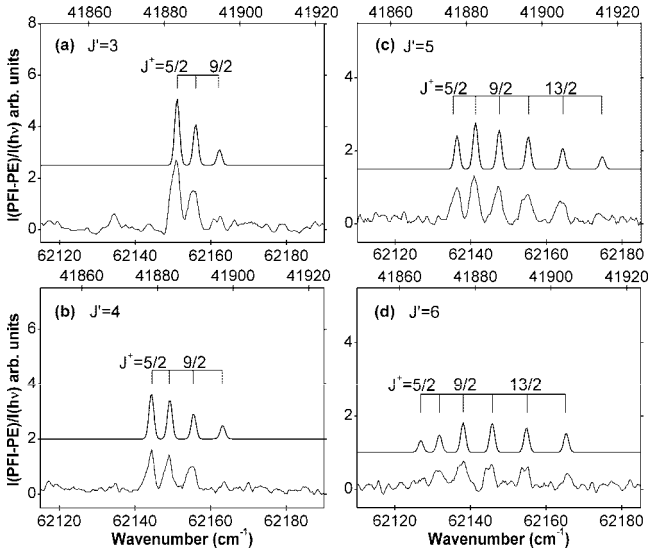

Figure 5. Rotationally selected and resolved PFI-PE spectra (lower spectra) for the formation of $FeC^+(X^2\Delta_{5/2}; v^+=1, J^+)$ from $FeC(^3\Delta_3; v'=0)$ with (a) $J' = 3$, (b) $J' = 4$, (c) $J' = 5$, and (d) $J' = 6$, which were selected by setting the ω_1 frequency at the respective $P(4)$, $P(5)$, $P(6)$, and $P(7)$ transition lines of the spectrum shown in Figure 1 and scanning the ω_2 frequency in the range of 41 850−41 922 cm^{-1} (top frequency scale). The total photon frequency range of 62 110−62 190 cm^{-1} is shown in the bottom frequency scale. The upper spectra are the simulated spectra.

the $v^+ = 0$ band of $FeC^+(X^2\Delta_{5/2})$. After taking into account the Stark shift, the band origin is determined to be $\upsilon_{00}{}^+ = 61\,245.1 \pm 0.5$ cm^{-1}. On the basis of the measured $B_0{}^+$ value, we have obtained the average $r_e{}^+$ value of 1.559 Å, which is found to be in excellent accord with the theoretical prediction[17] of 1.557 Å.

For photoionization transitions, the selection rules for total angular momentum changes from the neutral to the cation are $|\Delta J^+| = |J^+ - J'| \leq l + s + 1$, where l and s (=1/2) represent the orbital and spin angular momenta of the photoelectron. As pointed out above, the highest occupied molecular orbital for the excited intermediate $FeC(^3\Delta_3)$ state is the 4π-orbital. Thus, the ejected photoelectron from this orbital can give the maximum orbital angular momentum of $l = 2$, which corresponds to $|\Delta J^+| \leq 3.5$. This prediction is consistent with the ΔJ^+ observed in Figure 3, showing the maximum $|\Delta J^+| = 3.5$.

Parts a−d of Figure 5 show the state-to-state PFI-PE spectra (lower spectra) for the $FeC^+(X^2\Delta_{5/2}; v^+=1, J^+) \leftarrow FeC(^3\Delta_3; v'=0, J'=3,4,5,6)$ photoionization transitions in the total photon frequency range of 62 110−62 190 cm^{-1} (bottom frequency scale) obtained by setting the ω_1 frequency at the rotational transitions, $P(4)$, $P(5)$, $P(6)$, and $P(7)$, respectively, of the spectrum shown in Figure 1 and scanning the UV ω_2 frequency in the range of 41 850−41 922 cm^{-1} (top frequency scale). The upper spectra shown in parts a−d of Figure 5 are the simulated spectra, on top of which we have marked the J^+ rotational assignments from the selected $J' = 3$, 4, 5, or 6 rotational level of the $FeC(^3\Delta_3; v'=0)$ intermediate state. The rotational structures observed in Figure 5a−d are nearly identical with those found in Figure 4a−d, revealing that the $|\Delta J^+|$ changes are also limited to ≤3.5. On the basis of the least-squares fit according to the standard transition formula, we have obtained the rotational constant $B_1{}^+ = 0.6924 \pm 0.0009$ cm^{-1} and the Stark shift corrected band origin $\nu_{10}{}^+ = 62\,159.5 \pm 0.5$ cm^{-1} of the $v^+ = 1$ vibrational band of $FeC^+(X^2\Delta_{5/2})$.

We have also measured the PFI-PE spectrum for $FeC^+(X^2\Delta_{5/2}; v^+=1, J^+)$ (middle spectrum of Figure 6) in the total photon frequency range of 62 117−62 212 cm^{-1} (bottom frequency scale) by setting the ω_1 frequency at 20 278.67 cm^{-1} (the maximum of the R-branch of the spectrum shown in Figure 1) and scanning the ω_2 frequency in the range of 41 838−41 933 cm^{-1} (top frequency scale). The bottom PFI-PE spectrum of Figure 6 is obtained by summing the state-to-state PFI-PE spectra shown in Figure 5c,d, which represent the respective cross sections for the $FeC^+(X^2\Delta_{5/2}; v^+=1, J^+) \leftarrow FeC(^3\Delta_3; v'=0, J' = 5,6)$ photoionization transitions. The good agreement observed between the bottom PFI-PE spectrum and the middle experimental PFI-PE spectrum confirms the conclusion that the rotational levels of $FeC(^3\Delta_3; v'=0)$ prepared by setting ω_1 frequency at 20 278.67 cm^{-1} are predominantly the $J' = 5$ and 6 rotational levels. The top spectrum of Figure 6 represents the best simulated spectrum, and the rotational assignments based on the spectral simulation are marked on top of the simulated spectrum.

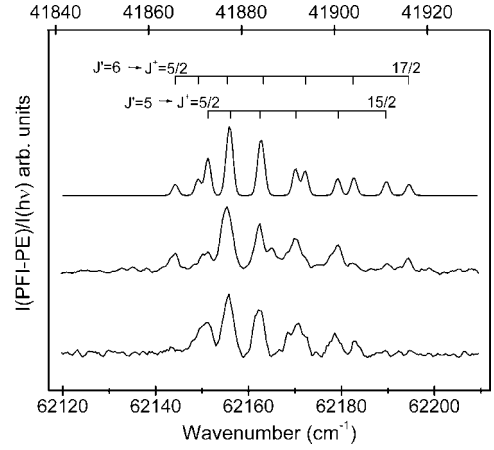

Figure 6. PFI-PE spectrum for $FeC^+(X^2\Delta_{5/2}; v^+=1, J^+)$ (middle spectrum) in the total photon frequency range of 62 117−62 212 cm^{-1} (bottom frequency scale) obtained by setting the ω_1 frequency at 20 278.67 cm^{-1} and scanning the ω_1 frequency in the range of 41 838−41 933 cm^{-1} (top frequency scale). The bottom spectrum is obtained by summing the PFI-PE spectra of parts c and d of Figure 5. The top spectrum represents the best simulated spectrum.

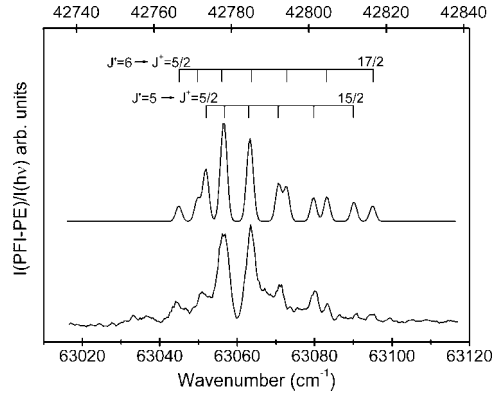

Figure 7. PFI-PE spectrum for $FeC^+(X^2\Delta_{5/2}; v^+=2, J^+)$ (lower spectrum) in the total photon frequency range of 63 010−63 120 cm^{-1} (bottom frequency scale) obtained by setting $\omega_1 = 20\,278.667$ cm^{-1} and scanning the ω_2 frequency in the range of 42 731−42 841 cm^{-1} (top frequency scale). The upper spectrum is the simulated spectrum.

The lower spectrum of Figure 7 depicts the PFI-PE spectrum for $FeC^+(X^2\Delta_{5/2}; v^+=2, J^+)$ in the total photon frequency range of 63 010−63 120 cm^{-1} (bottom frequency scale), which is obtained by setting the ω_1 frequency at 20 278.67 cm^{-1} and scanning the ω_2 frequency in the range of 42 731−42 841 cm^{-1}

(top frequency scale). The simulated spectrum is shown as the upper spectrum in Figure 7. As expected, the rotational structure of this PFI-PE spectrum for $FeC^+(X^2\Delta_{5/2};\ v^+=2,\ J^+)$ is similar to that of the PFI-PE spectrum for $FeC^+(X^2\Delta_{5/2};\ v^+=1,\ J^+)$ shown in Figure 6. Thus, the $J^+ \leftarrow J'$ rotational assignments of this spectrum are straightforward as marked on top of the simulated spectrum. The least-squares fit of the observed rotational peaks to the standard formula for rotational transitions yields the rotational constant $B_2{}^+ = 0.6845 \pm 0.0016\ cm^{-1}$ and the Stark shift corrected origin $\upsilon_{20}{}^+ = 63\,061.3 \pm 0.5\ cm^{-1}$ for the $v^+ = 2$ vibrational band of $FeC^+(X^2\Delta_{5/2})$.

The identification of the lowest rotational level to be $J^+ = 5/2$ in the $v^+ = 0$, 1, and 2 vibrational PFI-PE bands of Figures 4−7 shows that the angular momentum $\Omega^+ = 5/2$ for the FeC^+ ground state, and thus confirms that the cation ground state is $FeC^+(X^2\Delta_{5/2})$.[6,7] To our knowledge, no previous measurements on the vibrational and rotational constants of $FeC^+(X^2\Delta_{5/2})$ are available. By fitting the rotational constants $B_0{}^+$, $B_1{}^+$, and $B_2{}^+$ to the standard equation

$$B_v^+ = B_e^+ - \alpha_e^+(v^+ + 1/2) \qquad (2)$$

we have obtained the rotational constants $B_e{}^+ = 0.7015 \pm 0.0006\ cm^{-1}$ and $\alpha_e{}^+ = 0.00665 \pm 0.00036\ cm^{-1}$. The rotational and vibrational constants, together with the experimental $\upsilon_{00}{}^+$, $\upsilon_{10}{}^+$, and $\upsilon_{20}{}^+$ and $r_e{}^+$ value, for $FeC^+(X^2\Delta_{5/2})$ obtained in this study are listed in Table 1 for comparison with the ab initio theoretical predictions[17] based on the MRCI calculations. We note that the rotational constants determined here are effective rotational constants, which depend on the use of the phenomenological model eq 1. The rotational constants can be different if the spin−orbit interaction is small. Thus, the $B_v{}^+$ and $r_e{}^+$ values determined in the present study can have larger, systematic errors than the quoted statistical errors. As shown in Table 1, excellent agreement is observed between the rotational constants obtained here and the MRCI predictions. The experimental vibrational spacings measured as $\Delta G(v^+ + 1/2) = G(v^+ + 1) - G(v^+)$ for $v^+ = 0$ and 1 are of interest for comparison with theoretical predictions. Since the $\Delta G(1/2)$ and $\Delta G(3/2)$ values are measured by the frequency difference of the adjacent vibrational levels of the cation, their uncertainties are not influenced by the Stark shift effect. Thus, the $\Delta G(1/2) = 914.47 \pm 0.06\ cm^{-1}$ and $\Delta G(3/2) = 901.63 \pm 0.10\ cm^{-1}$ can be determined based on the $\upsilon_{00}{}^+$, $\upsilon_{10}{}^+$, and $\upsilon_{20}{}^+$ values before the Stark shift correction. As shown in Table 1, the $\Delta G(1/2)$ and $\Delta G(3/2)$ values obtained in the present study are lower than the respective theoretical MRCI predictions of 932.9 and 921.6 cm^{-1} by ~19 cm^{-1}.[17] On the basis of the measured $\Delta G(1/2)$ and $\Delta G(3/2)$ values, we have also obtained the vibrational constants $\omega_e{}^+ = 927.14 \pm 0.04\ cm^{-1}$ and $\omega_e{}^+\chi_e{}^+ = 6.35 \pm 0.04\ cm^{-1}$ for $FeC^+(X^2\Delta_{5/2};\ v^+=0-2)$, which are compared to the theoretical MRCI vibrational constants[17] $\omega_e{}^+ = 944.2\ cm^{-1}$ and $\omega_e{}^+\chi_e{}^+ = 5.64\ cm^{-1}$.

Defining the IE value of FeC [IE(FeC)] to be the transition energy from the lowest rovibrational level of the neutral $FeC(X^3\Delta_3)$ ground state to the lowest rovibrational level of the ionic $FeC^+(X^2\Delta_{5/2})$ ground state, i.e., $FeC^+(X^2\Delta_{5/2};\ v^+=0,\ J^+=5/2) \leftarrow FeC(X^3\Delta_3;\ v''=0,\ J''=3)$, we obtain the IE(FeC) = $61\,243.1 \pm 0.5\ cm^{-1}$ (7.59318 ± 0.00006 eV) after correction for the Stark shift. This value is 1185 cm^{-1} (0.147 eV) lower than the value of $62\,427 \pm 726\ cm^{-1}$ (7.74 ± 0.09 eV)[7] obtained previously by Brugh and Morse using the bracketing method. The IE values for the formation of $FeC^+(X^2\Delta_{5/2};\ v^+=1,2,\ J^+=5/2)$ from $FeC(X^3\Delta_3;\ v''=0,\ J''=3)$ are determined as 62 157.6 ± 0.5 and 63 059.2 ± 0.5 cm^{-1}, respectively. The IE values for the formation of $FeC^+(X^2\Delta_{5/2};\ v^+=0,1,2,3)$ determined by both the PFI-PE and PIE measurements are included in Table 1. The IE values determined by the PFI-PE measurement are more precise than those obtained from the PIE spectrum. Nevertheless, the IE determinations of 61 242 ± 5, 62 155 ± 5, and 63 051 ± 8 for the formation of $FeC^+(X^2\Delta_{5/2};\ v^+=0,1,2)$ from $FeC(X^3\Delta_3;\ v''=0)$ based on the PIE measurement are in good agreement those obtained by the analysis of the PFI-PE spectra of Figures 4−7 after taking into account the experimental uncertainties. The IE = $63\,939 \pm 10\ cm^{-1}$ for the formation of $FeC^+(X^2\Delta_{5/2};\ v^+=3)$ from $FeC(X^3\Delta_3;\ v''=0)$ has only been determined by the PIE measurement.

Due to the conservation of energy, we have the following relationsship: $D_0(Fe-C) + IE(Fe) = IE(FeC) + D_0(Fe^+-C)$. The IE(FeC) determined here, along with the known IE(Fe) =

TABLE 1: Comparison of Experimental and MRCI Theoretical Rotational and Vibrational Constants, 0 K Bond Dissociation Energies (D_0's), Ionization Energies (IEs) for $FeC^+(X^2\Delta_{5/2};\ v^+=0-3)$

$FeC^+(X^2\Delta_{5/2};\ v^+)$	exptl (this work)	theoretical (ref 17)
$v^+ = 0$		
$\upsilon_{00}{}^+$ (cm^{-1})[a]	61 245.1 ± 0.5	
IE (cm^{-1})[b]	61 243.1 ± 0.5	57 265
	61 242 ± 5[c]	
	62 427 ± 726[d]	
$B_0{}^+$ (cm^{-1})[e]	0.6978 ± 0.0008	0.7001
$v^+ = 1$		
$\upsilon_{10}{}^+$ (cm^{-1})[a]	62 159.5 ± 0.5	
IE (cm^{-1})[b]	62 157.6 ± 0.5	
	62 155 ± 5[c]	
$B_1{}^+$ (cm^{-1})[e]	0.6924 ± 0.0009	0.6937
$v^+ = 2$		
$\upsilon_{20}{}^+$ (cm^{-1})[a]	63 061.3 ± 0.5	
IE (cm^{-1})[b]	63 059.2 ± 0.5	
	63 051 ± 8[c]	
$B_2{}^+$ (cm^{-1})[e]	0.6845 ± 0.0016	0.6872
$v^+ = 3$		
IE (cm^{-1})[b]	63 939 ± 10[c]	
rotational constants		
$r_e{}^+$ (Å)[f]	1.559	1.557
$B_e{}^+$ (cm^{-1})[g]	0.7015 ± 0.0006	0.7033
$\alpha_e{}^+$ (cm^{-1})[g]	0.00665 ± 0.00036	0.00643
vibrational constants		
$\Delta G(1/2)$ (cm^{-1})[h]	914.47 ± 0.06	932.9
$\Delta G(3/2)$ (cm^{-1})[i]	901.63 ± 0.10	921.6
$\omega_e{}^+$ (cm^{-1})[j]	927.14 ± 0.04	944.2
$\omega_e{}^+\chi_e{}^+$ (cm^{-1})[j]	6.35 ± 0.04	5.64
bond dissociation energies		
$D_0(Fe^+-C) - D_0(Fe-C)$ (eV)[k]	0.309 ± 0.001	≈0[l]

[a] υ_{m0} represents the frequency difference between the $FeC^+(X^2\Delta_{5/2};\ v^+=m)$ and the $FeC(X^3\Delta_3;\ v'=0)$ states assuming both J^+ and $J' = 0$. [b] IE represents the energy difference between the $FeC^+(X^2\Delta_{5/2};\ v^+,\ J^+=5/2)$ and the $FeC(X^3\Delta_3;\ v'=0,\ J' = 3)$ states. [c] IE values determined by the PIE steps resolved in the PIE spectrum of Figure 3. [d] Reference 7. [e] $B_v{}^+$ represents the rotational constant the v^+ state. [f] Average equilibrium bond distance calculated based on the measured $B_0{}^+$ rotational constant. [g] Rotational constants obtained based on the best fit to the following equation: $B_v{}^+ = B_e{}^+ - \alpha_e(v^+ + 1/2)$. [h] Vibrational frequency spacing between the $v^+ = 0$ and 1 states. [i] Vibrational frequency spacing between the $v^+ = 1$ and 2 states. [j] Vibrational constants based on the following equation: $\Delta G(v^+ + 1/2) = G(v^+ + 1) - G(v^+) = \omega_e{}^+ - 2\omega_e{}^+\chi_e{}^+ - 2\omega_e{}^+\chi_e{}^+(v^+)$. [k] Difference in the 0 K bond dissociation energies for FeC [$D_0(Fe-C)$] and FeC^+ [$D_0(Fe^+-C)$]. [l] On the basis of the theoretical $D_0(Fe-C)$ and $D_0(Fe^+-C)$ predictions of 87 kcal/mol calculated at the C-MRCI level of theory were reported in refs 16 and . The latter studies also reported $D_0(Fe^+-C) = 92$ kcal/mol values calculated at the C-MRCI+Q level (see the text).

7.9024 ± 0.0001 eV (63,737.1 ± 0.8 cm^{-1}),[30] shows that the $D_0(Fe^+-C)$ is greater than $D_0(Fe-C)$ by 0.3094 eV. Ab initio quantum computation packages, such as the Gaussian-3 (G3) method, have been widely used for the calculation of energetic properties of main group species.[13,14] However, the G3 method is not applicable for the energetic prediction of transition metal-containing molecules because some basis sets for the transition metal atoms are unavailable for the G3 calculation.[13] We have obtained an IE(FeC) prediction of 7.8 eV with zero-point energy correction at the B3LYP/cc-pVTZ level of theory. To our knowledge, there have only been two[17,31] previous ab initio quantum calculations made on FeC^+. The most sophisticated ab initio quantum chemical calculations on FeC/FeC^+ have been the recent MRCI calculations of Tzeli and Mavridis performed at the C-MRCI+Q level of theory.[16,17] These calculations, which have taken into account the core-valence correlation effects, the Davidson correction, and scalar relativistic corrections, give the predictions for IE(FeC) = 7.10 eV.[17] There have been two measurements for $D_0(Fe^+-C)$, but these measurements differ by more than 10 kcal/mol and have large uncertainties.[32,33] The early measurement based on photodissociation yielded a $D_0(Fe^+-C)$ value of 94.5 ± 7 kcal/mol;[32] the recent determination based on synchrotron VUV dissociative photoionization[33] gives a value of 84.2 ± 4.1 kcal/mol. The MRCI calculations of Tzeli and Mavridis also give a wide range of D_0 values for FeC and FeC^+ at different levels of theory. They report a similar prediction of 87 kcal/mol for both $D_0(Fe^+-C)$ and $D_0(Fe-C)$ at the C-MRCI level of theory.[16,17] This prediction is inconsistent with the present experiment, which shows that $D_0(Fe^+-C)$ is larger than $D_0(Fe-C)$ by more than 0.309 eV. This, together with the large discrepancy observed between the experimental and theoretical values for the IE(FeC), points to the great need for further development of ab initio quantum computation procedures for more accurate energetic predictions of transition metal-containing molecules. We note that Itono et al. have earlier obtained a value of $D_0(Fe-C) = 81$ kcal/mol calculated at the ab initio multireference singles and doubles configuration interaction (MR-SDCI) molecular orbital method;[34] and Tzeli and Mavridis have also reported a value of $D_0(Fe^+-C) = 92$ kcal/mol[17,35] based on the C-MRCI+Q level. The Davidson correction is expected to be important for the FeC/FeC^+ system due to large size-nonextensivity errors inherent in the MRCI approach.[35] Obviously, the determination of highly precise experimental values for $D_0(Fe-C)$ and $D_0(Fe^+-C)$ would be very valuable for benchmarking the energetic predictions[16,17,34] of these ab initio quantum MRCI calculations.

IV. Conclusions

We have performed a two-color visible−UV PIE and PFI-PE study of FeC prepared by using a laser ablation metal beam source. By selecting specific J' rotational levels of the intermediate FeC($^3\Delta_3$; $v'=0$) state by visible laser excitation, followed by UV laser photoionization, we have obtained the rotationally resolved photoelectron vibrational bands for $FeC^+(X^2\Delta_{5/2}; v^+ = 0,1,2)$. The complete resolution of rotational transitions has allowed the unambiguous rotational assignments of the PFI-PE bands, yielding precise determinations for the IE(FeC) and rotational and vibrational constants for $FeC^+(X^2\Delta_{5/2}; v^+=0-2)$. These experimental values have been used to benchmark the recently high-level ab initio quantum calculations performed at the C-MRCI+Q level,[16,17] The discrepancies observed between the present PFI-PE results and the C-MRCI+Q calculations point to the need for further development of ab initio quantum computation procedures for more reliable energetic predictions of transition metal-containing molecules.

Acknowledgment. C.Y.N. is grateful for helpful discussions with Prof. Dong-Sheng Yang, Prof. Timothy C. Steimle, and Prof. Michael Morse concerning the design and operation of the laser ablation metal beam source. This work was supported by NSF Grant No. CHE 0517871. Partial support by the DOE Contract No. DE-FG02-02ER15306, the AFOSR Grant No. FA9550-06-1-0073, and the NASA Grant No. 07-PATM07-0012 is also gratefully acknowledged.

References and Notes

(1) Harrison, J. F. *Chem. Rev.* **2000**, *100*, 679–716, and references cited therein.
(2) Merer, A. J. *Annu. Rev. Phys. Chem.* **1989**, *40*, 407, and references cited therein.
(3) Landolt-Börnstein *Astronomy and Astrophysics*; New Series Group 6, Vol. 1; Spring-Verlag: Berlin, Germany, 1965.
(4) Allen, M. D.; Pesch, T. C.; Ziury, L. M. *Astrophys. J.* **1996**, *472*, L57.
(5) Thomas, J. M.; Johnson, B. F. G.; Raja, R.; Sankar, G.; Midgley, P. A. *Acc. Chem. Res.* **2003**, *36*, 20.
(6) Balfour, W. J.; Cao, J.; Prasad, C. V. V.; Qian, C. X. W. *J. Chem. Phys.* **1995**, *103* (10), 4046.
(7) Brugh, D. J.; Morse, M. D. *J. Chem. Phys.* **1997**, *107* (23), 9772.
(8) Leung, J. W.-H.; Tam, W. S.; Ran, Q.; Cheung, A. S.-C. *Chem. Phys. Lett.* **2001**, *343*, 64.
(9) Huber, K. P.; Herzberg, G. *Constants of Diatomic Molecules*; Van Nostrand Reinhold: New York, 1979.
(10) Harrington, J.; Weisshaar, J. C. *J. Chem. Phys.* **1992**, *97*, 2809.
(11) Linton, C.; Simard, B.; Loock, H. P.; Wallin, S.; Rothschopf, G. K.; Gunion, R. F.; Morse, M. D.; Armentrout, P. B. *J. Chem. Phys.* **1999**, *111*, 5017.
(12) Loock, H.; Simard, B.; Wallen, S.; Linton, C. *J. Chem. Phys.* **1998**, *109*, 8980.
(13) Raghavachari, K.; Curtiss, L. A. In *Understanding Chemical Reactivity: Quantum-Mechanical Prediction of Thermochemical Data*; Ciosolwski, J., Ed.; Kluwer Academic Publishers: New York, 2001; Vol. 22, pp 67−95 andreferences cited therein.
(14) Martin, J. M. L.; Parthiban, S. In *Understanding Chemical Reactivity: Quantum-Mechanical Prediction of Thermochemical Data*; Ciosolwski, J., Ed.; Kluwer Academic Publishers: New York, 2001; Vol. 22, pp 31−62 andreferences cited therein.
(15) Lau, K.-C.; Ng, C. Y. *Acc. Chem. Res.* **2006**, *39*, 823–829.
(16) Tzeli, D.; Mavridis, A. *J. Chem. Phys.* **2002**, *116*, 4901.
(17) Tzeli, D.; Mavridis, A. *J. Phys. Chem. A* **2005**, *109*, 9249.
(18) Wang, P.; Xing, X.; Lau, K C.; Woo, H. K.; Ng, C. Y. *J. Chem. Phys.* **2004**, *121*, 7049.
(19) Ng, C. Y. *J. Electron Spectrosc. Relat. Phenom.* **2004**, *152*, 142.
(20) Xing, X.; Bahng, M.-K.; Wang, P.; Lau, K. C.; Baek, S.-J.; Ng, C. Y. *J. Chem. Phys.* **2006**, *125*, 133304.
(21) Xing, X.; Bahng, M.-K.; Reed, B.; Lam, C. S.; Lau, K. C.; Ng, C. Y. *J. Chem. Phys.* **2008**, *128*, 094311.
(22) Xing, X.; Reed, B.; Bahng, M.-K.; Baek, S. J.; Wang, P.; Ng, C. Y. *J. Chem. Phys.* **2008**, *128*, 104306.
(23) Xing, X.; Wang, P.; Woo, H.-K.; Bahng, M.-K.; Baek, S.-J.; Ng, C. Y. *Chem. Phys. Lett.* **2008**, *455*, 321.
(24) Xing, X; Reed, B.; Bahng, M.-K.; Ng, C. Y. *J. Phys. Chem. A* **2008**, *112*, 9277.
(25) Ng, C. Y. In *Frontiers of Molecular Spectroscopy*; Laane, J., Ed.; Elsevier Science and Technology: New York, 2008; Vol. *19*, pp 659−691.
(26) Xing, X.; Reed, B.; Bahng, M.-K.; Wang, P.; Woo, H.-K.; Baek, S.-J.; Lam, C. S.; Ng, C. Y. *Chin. J. Chem. Phys.* **2008**, *21*, 193.
(27) Woo, H. K.; Lau, K. C.; Zhan, J. P.; Ng, C. Y.; Li, C. L.; Li, W. K.; Johnson, P. M. *J. Chem. Phys.* **2003**, *119*, 7789.
(28) Woo, H. K.; Wang, P.; Lau, K.-C.; Xing, X.; Ng, C. Y. *J. Chem. Phys.* **2004**, *120*, 9561.
(29) Dietz, T. G.; Duncan, M. A.; Powers, D. E.; Smalley, R. E. *J. Chem. Phys.* **1981**, *74*, 6511.
(30) *NIST Atomic Spectra Database*, version 3.1.5, 2008: http://physics.nist.gov/asd3.
(31) Gutsev, G. L.; Bauschlicher, C. W., Jr. *Chem. Phys.* **2003**, *291*, 27.
(32) Hettich, R. L.; Freiser, B. S. *J. Am. Chem. Soc.* **1986**, *108*, 2537.
(33) Angeli, A.; Berthier, G.; Rolando, C.; Sablier, M.; Alcaraz, C.; Dutuit, O. *J. Phys. Chem. A* **1997**, *101*, 7907.
(34) Itono, S. S.; Taketsugu, T.; Hirano, T.; Nagashima, U. *J. Chem. Phys.* **2001**, *115*, 11213.
(35) A. Mavridis, private communication.

JP810797V